Article

Neuron

Inhibitory and Excitatory Spike-Timing-Dependent Plasticity in the Auditory Cortex

Highlights

- Spike pairing induces STDP of excitatory and inhibitory layer 5 cortical synapses
- Inhibitory potentiation occurs when either pre- or postsynaptic spikes come first
- Inhibitory potentiation depends on the initial excitatory-inhibitory ratio
- Excitatory and inhibitory inputs become bound together by postsynaptic spiking

Authors

James A. D'amour, Robert C. Froemke

Correspondence

robert.froemke@med.nyu.edu

In Brief

D'amour and Froemke show how inhibitory and excitatory synapses are co-modified by pre- and postsynaptic spike pairing. Inhibitory plasticity depends on the initial excitatory-inhibitory ratio to help balance inhibition with excitation.

D'amour & Froemke, 2015, Neuron *86*, 514–528
April 22, 2015
http://dx.doi.org/10.1016/j.neuron.2015.03.014

CellPress

CellPress

Neuron
Article

Inhibitory and Excitatory Spike-Timing-Dependent Plasticity in the Auditory Cortex

James A. D'amour[1,2] and Robert C. Froemke[1,2,*]
[1]Molecular Neurobiology Program, The Helen and Martin Kimmel Center for Biology and Medicine at the Skirball Institute for Biomolecular Medicine, Neuroscience Institute, Departments of Otolaryngology, Neuroscience and Physiology, New York University School of Medicine, 540 First Avenue, New York, NY 10016, USA
[2]Center for Neural Science, New York University, 4 Washington Place, New York, NY 10003, USA
*Correspondence: robert.froemke@med.nyu.edu
http://dx.doi.org/10.1016/j.neuron.2015.03.014

SUMMARY

Synapses are plastic and can be modified by changes in spike timing. Whereas most studies of long-term synaptic plasticity focus on excitation, inhibitory plasticity may be critical for controlling information processing, memory storage, and overall excitability in neural circuits. Here we examine spike-timing-dependent plasticity (STDP) of inhibitory synapses onto layer 5 neurons in slices of mouse auditory cortex, together with concomitant STDP of excitatory synapses. Pairing pre- and postsynaptic spikes potentiated inhibitory inputs irrespective of precise temporal order within ~10 ms. This was in contrast to excitatory inputs, which displayed an asymmetrical STDP time window. These combined synaptic modifications both required NMDA receptor activation and adjusted the excitatory-inhibitory ratio of events paired with postsynaptic spiking. Finally, subthreshold events became suprathreshold, and the time window between excitation and inhibition became more precise. These findings demonstrate that cortical inhibitory plasticity requires interactions with co-activated excitatory synapses to properly regulate excitatory-inhibitory balance.

INTRODUCTION

Synaptic plasticity is a fundamental feature of the CNS, especially for the function of the neocortex and other neural circuits involved in learning, memory, and similar cognitive processes (Carcea and Froemke, 2013; Frankland et al., 2001; Hebb, 1949; McClelland et al., 1995). In particular, adjustments of excitatory synaptic strength are believed to be a major mechanism by which cortical networks adapt to the statistics of sensory input, over a range of timescales from seconds to days (Buonomano and Merzenich, 1998; Froemke and Martins, 2011; Martin et al., 2000; McGaugh 2000). Earlier studies of synaptic plasticity in cortex and hippocampus examined how induction of long-term potentiation (LTP) and long-term depression (LTD) depended on the overall rate of electrical stimulation (Bienenstock et al., 1982; Bliss and Collingridge, 1993; Kirkwood et al., 1993; Malenka and Nicoll, 1999). More recent work, however, has focused on the importance of precise timing of pre- and postsynaptic action potentials for induction of spike-timing-dependent plasticity (STDP) at unitary connections (Bi and Poo, 1998; Debanne et al., 1994; Markram et al., 1997; Sjöström et al., 2001) and excitatory inputs evoked by extracellular stimulation (Bell et al., 1997; Feldman, 2000; Froemke and Dan, 2002). Across most (but not all) cell types, brain areas, and species, a general rule has emerged for STDP of excitatory synapses: when presynaptic neurons fire within approximately 10–20 ms before postsynaptic spiking (pre→post pairing), LTP is induced, but when the postsynaptic cell fires first (post→pre pairing) within 20–100 ms, LTD is induced (Dan and Poo, 2006, Feldman, 2012, Froemke et al., 2010; Markram et al., 2011).

The learning rules for inhibitory synapses are less clear (Lamsa et al., 2010; Vogels et al., 2013). There have been some studies of inhibitory plasticity; for example, during early cortical development when GABAergic synapses are depolarizing (Woodin et al., 2003), in hippocampus (Gaiarsa et al., 2002; Ormond and Woodin, 2011), entorhinal cortex (Haas et al., 2006), and sensory cortex (Holmgren and Zilberter, 2001; Komatsu, 1994; Maffei et al., 2006; Wang and Maffei, 2014). There is some agreement as to mechanisms involved in GABAergic synaptic plasticity, in that postsynaptic Ca^{2+} influx through L-type channels has been implicated in several studies (Haas et al., 2006; Ormond and Woodin, 2011), and there is a growing body of literature about the modifications to GABA receptors and Cl^- transport systems that affect inhibitory synaptic strength and expression of inhibitory plasticity (Kullmann et al., 2012; Lamsa et al., 2010). However, there is less consensus about the relations between activity patterns and induction of various forms of inhibitory plasticity. Whereas this may be due to the heterogeneity of cortical inhibitory cell types (DeFelipe et al., 2013; Fishell and Rudy, 2011), this may also be confounded by examining inhibition outside of its main context; namely, regulation of excitatory input and postsynaptic action potential generation.

Here we take a different strategy and examine inhibitory STDP together with excitatory STDP in the same cortical neurons. These experiments were motivated by in vivo studies that have consistently reported co-tuned and correlated patterns of excitation and inhibition in a number of systems, including the rodent auditory cortex (Froemke et al., 2007; Tan and Wehr, 2009; Volkov and Galazjuk, 1991; Wehr and Zador, 2003). This fine-scale

balance between stimulus-evoked excitation and inhibition is thought to be critical for control of precise spike timing, network activity, synaptic plasticity, and seizure generation (Carcea and Froemke, 2013; Hensch and Fagiolini, 2005; Wehr and Zador, 2003). Intriguingly, co-tuned inhibitory responses are not present upon birth or hearing onset, but develop in an activity- and experience-dependent manner over the first few weeks of postnatal life (Chang et al., 2005; Dorrn et al., 2010). Excitatory-inhibitory balance is also transiently disrupted in the adult cortex by cholinergic modulation (Kruglikov and Rudy, 2008; Letzkus et al., 2011; Metherate and Ashe, 1993) to enable long-term changes in frequency tuning curve structure and perceptual learning (Froemke et al., 2007, 2013). It remains unknown how inhibitory inputs are shaped by neural activity to balance or re-balance excitation. This problem is especially challenging because excitatory inputs are highly plastic, and populations of excitatory synapses can be modified within seconds to minutes after periods of patterned stimulation and/or elevated neuromodulatory tone. Inhibitory synapses must somehow track these changes, and be rapidly and accurately re-weighted to control excitability.

A recent theoretical study of receptive field plasticity in the auditory cortex suggested that inhibitory STDP can appropriately modify inhibitory synaptic strength in proportion with simultaneously stimulated excitatory inputs, leading to the emergence or return of fine-scale excitatory-inhibitory balance (Vogels et al., 2011). Thus our goal was to examine excitatory and inhibitory STDP together, to determine the learning rules required to jointly modify both excitation and inhibition in a way that preserves or enforces co-tuning. We found that the requirements for inhibitory LTP were similar to those postulated by Vogels et al. (2011). Surprisingly, however, we also found that this inhibitory plasticity depended on NMDA receptor activation and led to a normalization of the relationship between excitatory and inhibitory inputs co-activated with postsynaptic spiking. Thus, initially mismatched excitatory and inhibitory inputs can become co-tuned simply by coincident pre- and postsynaptic spiking.

RESULTS

Measuring Excitation and Inhibition in Mouse Auditory Cortical Neurons

To examine synaptic transmission and plasticity of cortical inhibitory and excitatory synapses together, we made whole-cell recordings from layer 5 pyramidal neurons in brain slices of mouse auditory cortex from animals postnatal day (P) 10–26 (Figure 1A). Cells were held in voltage-clamp at two membrane potentials alternating between −40 mV to measure inhibitory postsynaptic currents (IPSCs) and −80 mV to measure excitatory postsynaptic currents (EPSCs) evoked with an extracellular stimulation electrode placed within 150 μm of the recorded cell, generally near the apical dendrite in layer 4 (Figure 1B). Although measurements of synaptic strength were performed in voltage-clamp, spikes were not blocked (i.e., internal solution did not contain QX-314), so that we might elicit action potentials for studies of STDP.

Some of these events evoked at −80 or −40 mV were isolated inward or outward currents (Figures 1B and 1C). In many cases, though, evoked responses were a mixture of inward and outward currents, particularly at −40 mV. To ensure that we could reliably measure the excitatory and inhibitory components of these responses, we examined timing differences between peak inward and outward currents, the reversal potentials of these peaks, and pharmacological sensitivity.

For example, two different recordings showing inward and outward currents evoked at multiple holding potentials are displayed in Figures S1A and S1B. In each case, the peak inward and outward currents were clearly separable in time, and reversed at distinct holding potentials. Similar observations were made for all recordings included in this study (Figures S1C–S1E), giving us confidence that inward currents represented EPSCs that reversed at approximately −30 mV and outward currents represented IPSCs that reversed at approximately −70 mV. Inward currents were reliably elicited several milliseconds before the onset of outward currents (Figure S1C), consistent with previous studies by Gil and Amitai (1996), who found that layer 5 neurons in slices from barrel cortex respond to extracellular stimulation with early excitation followed by delayed inhibition on a similar timescale.

We confirmed that IPSCs were blocked by the GABA receptor antagonist picrotoxin (10–50 μM) and EPSCs were blocked by the AMPA receptor antagonist DNQX (25 μM) washed into the bath solution (Figure 1C). DNQX reduced inward currents at −70 mV almost to zero, but had a much more modest effect on outward currents measured at −40 mV (Figure S2; currents in four of ten cells were not significantly enhanced). Regardless, it is important to note that in general, events evoked at −40 mV were not purely inhibitory. In particular, across individual recordings, stimulation evoked a varying degree of inhibition relative to excitation. In some cases this excitatory-inhibitory ratio (E/I ratio) might be quite high if only a small amount of inhibition was evoked (these events would be more susceptible to DNQX and have reversal potentials closer to −70 mV), and in other recordings the E/I ratio might be low if inhibition dominated (and thus these events would be less susceptible to DNQX and have reversal potentials depolarized from −70 mV).

Finally, the reversal potentials for outward currents were stable over the age range studied here (P10–P26) and consistently at approximately −70 mV, similar to the reversal potentials measured in neurons from adult animals (Figure S1F). Thus by P10, GABAergic reversal potential is similar to that of adults in the mouse auditory cortex. This is perhaps a few days earlier than that reported for rat somatosensory cortex and visual cortex in vitro (Luhmann and Prince, 1991; Owens et al., 1996), possibly because of the early critical periods in rodent auditory cortex (de Villers-Sidani et al., 2007; Dorrn et al., 2010). Although spike pairing protocols at immature synapses transform depolarizing GABAergic responses into hyperpolarizing responses via changes in reversal potential (Lamsa et al., 2010; Woodin et al., 2003), we focused on examining how inhibitory strength could be modified once GABAergic reversal potential reached mature levels.

Spike Pairing at Short Intervals Induced Inhibitory LTP

After measuring baseline synaptic strength for 5–20 min, recordings were switched to current-clamp in order to pair inhibitory and/or excitatory postsynaptic potentials (IPSPs or EPSPs)

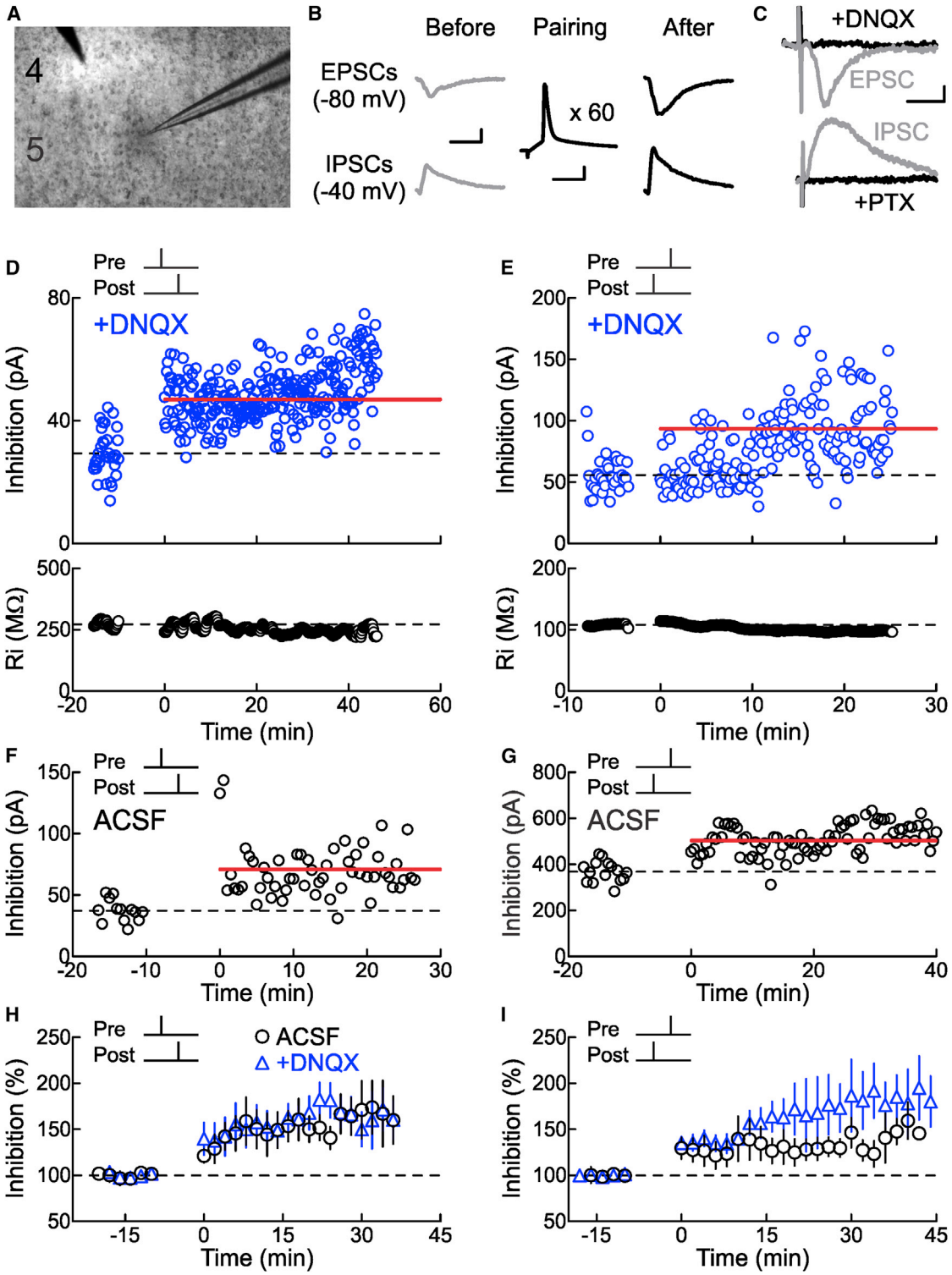

Figure 1. Inhibitory STDP Induced by Repetitive Spike Pairing in Auditory Cortex

(A) Whole-cell recording from layer 5 pyramidal neuron of mouse auditory cortex in brain slice.

(B) Experimental design. Extracellular stimulation evoked EPSCs and IPSCs monitored at −80 mV and −40 mV, respectively, in voltage-clamp before and after pairing. Scale: 10 ms, 100 pA. During pairing, recordings were switched to current-clamp to allow postsynaptic cells to fire single action potentials paired with single extracellular shocks (60 pairings, 0.1–0.2 Hz). Scale: 5 ms, 20 mV.

(C) Picrotoxin (20 μM) blocked IPSCs evoked at −40 mV. In a different recording, DNQX (25 μM) blocked EPSCs evoked at −80 mV. Scale: 15 ms, 10 pA.

(legend continued on next page)

with postsynaptic spiking induced by depolarization through the whole-cell electrode (Figure 1B). A single shock of extracellular stimulation was paired with a single postsynaptic action potential at a certain fixed timing interval between pre- and postsynaptic activity (Δt), and this pairing was repeated for 5–10 min a total of 60 times at 0.1–0.2 Hz (Froemke and Dan, 2002). After pairing, recordings were returned to the voltage-clamp and monitored for as long as input resistance (R_i) and series resistance (R_s) remained stable.

We found that spike pairing induced LTP of inhibitory synapses for short pairing intervals ($-10 \leq \Delta t \leq 10$ ms) regardless of the temporal order of the pre- and postsynaptic action potentials. First, we examined STDP of monosynaptic inhibitory synaptic responses isolated with DNQX. An example of inhibitory LTP induced by pre→post pairing is shown in Figure 1D. Initially, the mean baseline IPSC amplitude before pairing was 29.3 ± 1.3 pA. Single postsynaptic spikes were then paired with single IPSPs at an interval of Δt = 2 ms, and 16–25 min after pairing the mean IPSC amplitude increased by 60% to 46.9 ± 0.9 pA. Likewise, inhibitory LTP was also induced by post→pre pairing, as observed in the example cell shown in Figure 1E ($\Delta t = -5$ ms, IPSC before: 55.8 ± 2.5 pA, IPSC after: 93.3 ± 3.5 pA, increase of 67% after pairing).

Similar modifications of IPSCs were induced by pre/post pairing without DNQX in the bath, indicating that inhibitory STDP can be independent of AMPA receptor transmission. Example recordings with pre→post pairing and post→pre pairing in control ACSF are shown in Figures 1F and 1G, respectively. Inhibitory LTP in the presence or absence of DNQX are summarized in Figure 1H for short interval pre→post pairing ($0 \leq \Delta t \leq 10$ ms; 27/37 cells showed significant inhibitory LTP) and Figure 1I for short interval post→pre pairing ($-10 \leq \Delta t < 0$ ms; 24/36 cells showed significant inhibitory LTP).

Time Windows for Inhibitory and Excitatory STDP

We next examined STDP of excitatory inputs onto these neurons (Figure 2). As expected for cortical excitatory synapses, short interval pre→post pairing induced LTP, both when inhibition was intact or blocked with picrotoxin (Figures 2A, 2C, and 2E; 26/46 cells showed significant excitatory LTP in ACSF, 5/12 cells showed significant excitatory LTP in 10 μM picrotoxin), while short interval post→pre pairing induced LTD (Figures 2B, 2D, and 2F; 28/38 cells showed significant excitatory LTD in ACSF, 6/7 cells showed significant excitatory LTD in picrotoxin). Thus, pre→post pairing leads to a substantial enhancement of synaptic strength for both excitation and inhibition. This ensures that inhibitory responses approximately balance excitatory inputs that are reliably co-activated together, after those excitatory synapses are strengthened. Conversely, post→pre pairing increases inhibition while weakening excitation, providing a synergistic mechanism for enforcing reductions in excitability by co-active inputs that have repetitively failed to evoke postsynaptic spiking.

The time windows for changes to inhibitory and excitatory synapses onto layer 5 pyramidal cells in mouse auditory cortex are shown in Figure 3. The magnitude of inhibitory LTP could in some cases be quite large (Figure 3A). Outside of the short pairing interval ($-10 \leq \Delta t \leq 10$ ms), little to no long-term synaptic modification was observed for inhibition (Figure 3A), although longer post→pre timings also seemed to produce some excitatory LTD (Figure 3B).

Thus, while the time window for excitatory STDP at these synapses is conventionally asymmetrical (i.e., a shorter window for LTP induced by pre→post pairing and a longer window for LTD induced by post→pre pairing), the time window for inhibitory STDP is symmetrical around coincident pre- and postsynaptic spiking within a short interval. This symmetrical window for inhibitory STDP is similar in shape to a learning rule for inhibitory synapses recently proposed by Vogels et al. (2011) in their modeling study of excitatory-inhibitory balance.

Inhibitory and Excitatory STDP Both Required NMDA Receptors

We examined the mechanistic requirements for induction of inhibitory and excitatory STDP. Surprisingly, it appeared that both forms of synaptic plasticity involved a shared set of components: NMDA receptors and L-type Ca^{2+} channels (Figure 4). Although inhibitory STDP could be induced when AMPA receptors were blocked with DNQX (Figures 1 and 3A, blue triangles), blocking NMDA receptors with APV (50 μM) prevented spike pairing from modifying either excitatory or inhibitory events. An example cell where EPSCs and IPSCs were both monitored in the presence of APV is shown in Figure 4A. Pre→post pairing (Δt = 3 ms) had no effect on synaptic strength in this cell. Whereas excitatory plasticity is known to generally require NMDA receptor activation (Malenka and Nicoll, 1999; Feldman 2012), it is surprising that GABAergic synaptic plasticity also required co-activation of these glutamate receptors.

(D) Example of inhibitory spike-timing-dependent LTP induced by pre→post pairing. IPSCs were isolated in ACSF containing DNQX. Top, IPSC strength before and after pairing (Δt = 2 ms, before pairing: 29.3 ± 1.3 pA, 16–25 min after pairing: 46.9 ± 0.9 pA, increase of 60%). Dashed line, mean IPSC amplitude before pairing. Red bar, mean IPSC amplitude 16–25 min after pairing. Bottom, R_i for this cell (before, 272.1 ± 2.5 MΩ; after, 250.2 ± 1.5 MΩ; change of −8.1%).
(E) Example of inhibitory LTP induced by post→pre pairing in DNQX. Top, IPSC strength before and after pairing ($\Delta t = -5$ ms, before: 55.8 ≥ 2.5 pA, after: 93.3 ± 3.5 pA, increase of 67%). Bottom, R_i (before, 107.9 ± 0.3 MΩ; after, 97.3 ± 0.3 MΩ; change of −9.8%).
(F) Example of inhibitory LTP induced by pre→post pairing in normal ACSF (Δt = 4 ms: before, 37.3 ± 2.5 pA; after: 70.9 ± 2.8 pA, increase of 90%).
(G) Example of inhibitory LTP induced by post→pre pairing in ACSF ($\Delta t = -3.8$ ms: before, 368.3 ± 11.7 pA; after, 503.0 ± 10.0 pA; increase of 37%).
(H) Summary of short interval ($0 \leq \Delta t \leq 10$ ms) pre→post pairing experiments on IPSC amplitude. Circles, experiments in ACSF (increase of 51.4% ± 13.4%, n = 28, p < 0.0005; 19/28 cells showed significant inhibitory LTP); blue triangles, experiments in DNQX (increase of 71.1% ± 17.1%, n = 9, p < 0.0002; eight of nine cells showed significant inhibitory LTP). Error bars represent mean ± SEM.
(I) Summary of short interval ($-10 \leq \Delta t < 0$ ms) post→pre pairing experiments on IPSC amplitude. Circles, experiments in ACSF (increase of 27.9% ± 9.8%, n = 25, p < 0.0001; 17/25 cells showed significant inhibitory LTP); blue triangles, experiments in DNQX (increase of 66.5% ± 17.8%, n = 11, p < 0.00001; 7/11 cells showed significant inhibitory LTP). Error bars represent mean ± SEM.

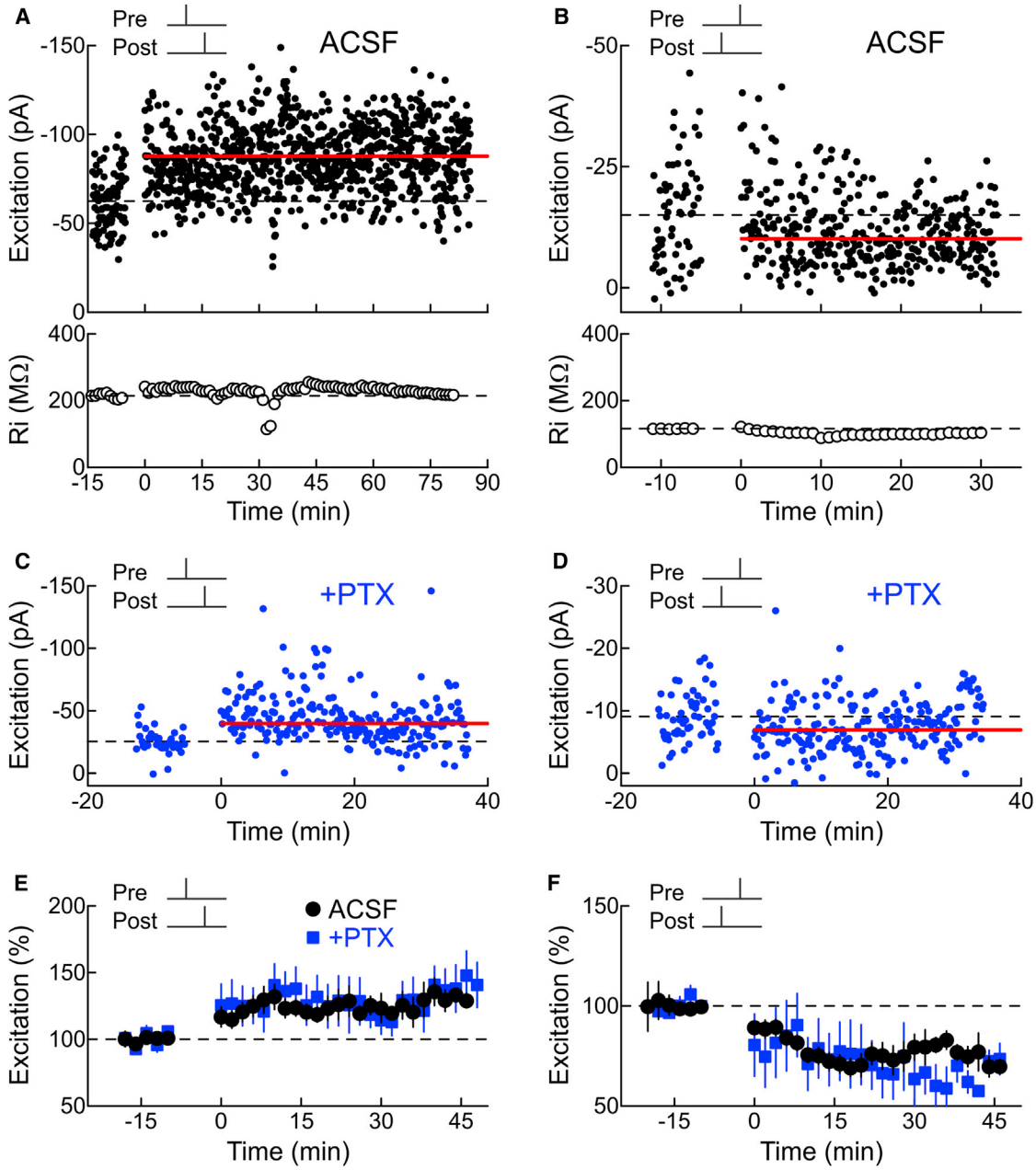

Figure 2. Excitatory STDP in Auditory Cortex

(A) Spike-timing-dependent excitatory LTP induced by short interval pre→post pairing in ACSF. Top, example recording monitoring EPSC strength before and after pairing ($\Delta t = 0$ ms: before, −62.5 ± 1.5 pA; after, −87.7 ± 1.7 pA; increase of 40.4%). Dashed line, mean EPSC amplitude before pairing. Red bar, mean EPSC amplitude 16–25 min after pairing. Bottom, R_i for this cell (before, 214.1 ± 2.3 MΩ; after, 225.0 ± 0.9 MΩ; change of 5.1%).

(B) Excitatory LTD induced by post→pre pairing in ACSF. Top, example recording monitoring EPSCs before and after pairing ($\Delta t = -5$ ms: before, −15.0 ± 1.2 pA; after, −10.1 ± 0.6 pA, decrease of −32.7%). Bottom, R_i (before, 115.9 ± 0.4 MΩ; after, 99.0 ± 0.1 MΩ; change of −14.6%).

(C) Example of excitatory LTP induced by pre→post pairing in picrotoxin (10 μM PTX, $\Delta t = 5$ ms: before, −25.3 ± 1.4 pA; after, −39.7 ± 2.0 pA; increase of 57%).

(D) Example of excitatory LTD induced by post→pre pairing in picrotoxin ($\Delta t = -5$ ms: before, −9.1 ± 0.5 pA; after, −6.9 ± 0.5 pA; decrease of 24%).

(E) Summary of short interval ($0 \leq \Delta t \leq 10$ ms) pre→post pairing experiments on excitation. Circles, experiments in ACSF (increase of 23.4% ± 6.4%, n = 46, $p < 0.0002$; 26/46 cells showed significant excitatory LTP); blue squares, experiments in picrotoxin (increase of 29.3% ± 14.0%, n = 12, $p < 0.05$; 5/12 cells showed significant excitatory LTP). Error bars represent mean ± SEM.

(F) Summary of short interval ($-10 \leq \Delta t < 0$ ms) post→pre pairing experiments on excitation. Circles, experiments in ACSF (decrease of −27.7% ± 4.4%, n = 38, $p < 0.0001$; 28/38 cells showed significant excitatory LTD); blue squares, experiments in picrotoxin (decrease of 38.9% ± 11.8%, n = 7, $p < 0.007$; six of seven cells showed significant excitatory LTD). Error bars represent mean ± SEM.

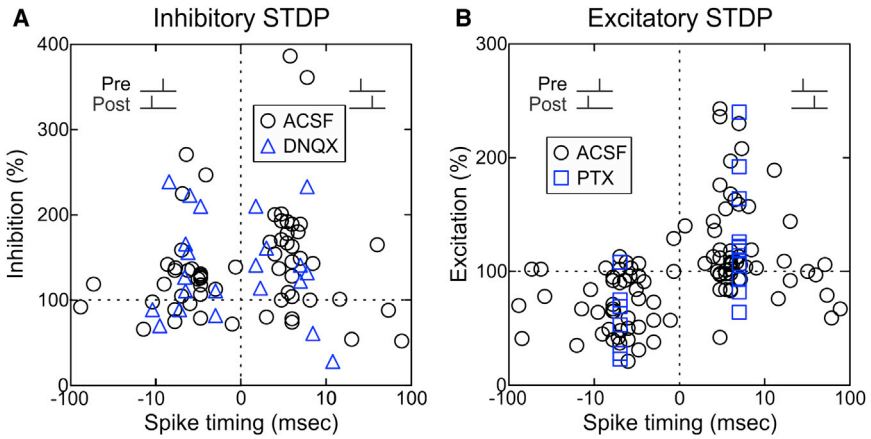

Figure 3. Time Windows for Induction of Inhibitory and Excitatory STDP

(A) Time window for inhibitory STDP (pre→post pairing, n = 43; post→pre pairing, n = 41). Circles, ACSF (n = 62). Triangles, DNQX (n = 22). Measurements of synaptic strength were computed 16–25 min after pairing.

(B) Time window for excitatory STDP (pre→post pairing, n = 69; post→pre pairing, n = 53). Circles, ACSF (n = 103). Squares, picrotoxin (PTX; n = 19).

Long-term modification of other GABAergic synapses has been found to require L-type Ca^{2+} channels (Haas et al., 2006; Ormond and Woodin, 2011). Similarly, we found that both excitatory and inhibitory STDP were prevented by nimodipine. An example cell is shown in Figure 4B, and these pharmacological experiments with APV or nimodipine are summarized in Figure 4C (for inhibitory STDP; filled bars, pre→post pairing; open bars, post→pre pairing) and Figure 4D (for excitatory STDP).

STDP Enhanced Postsynaptic Spike Firing

What are the functional consequences of combined inhibitory and excitatory STDP? We asked how these changes to excitation and inhibition might contribute to action potential generation, in two ways. First, we determined the effects of pre→post pairing on action potential generation directly. Although excitatory LTP induced by pre→post pairing should enhance the likelihood of spike firing in response to paired inputs, concomitant inhibitory LTP might prevent a sizable increase of postsynaptic spiking or possibly prevent action potential production if inhibitory events become large. We also examined the interval between EPSC and IPSC onset, as a measure of the time window (E-I window) during which postsynaptic cells can integrate excitatory inputs before inhibition curtails spiking (Kruglikov and Rudy, 2008).

We made current-clamp recordings from layer 5 pyramidal neurons, slightly depolarizing these cells so that extracellularly evoked EPSPs occasionally but infrequently elicited spikes during the baseline period. In the cell shown in Figure 5A, initial spiking probability was 0.54. After pre→post pairing, EPSPs were potentiated by 23% and spiking probability increased to 1.0 (spikes were evoked on every trial). Similar increases of spike probability after pre→post pairing were observed in seven of nine cells (Figure 5B).

Conversely, post→pre pairing could reduce spiking probability. In other experiments where the baseline strength in current-clamp was higher, synaptic responses produced spikes on a substantial number of trials before pairing (Figures 5C and 5D). After post→pre pairing, however, the probability of spike generation decreased (Figures 5C and 5D; seven of eight cells showed significant decreases in spiking); this is likely a consequence of the combination of excitatory LTD and inhibitory LTP induced by post→pre pairing.

We then made voltage-clamp recordings, holding cells at a range of different holding potentials (−40 to −80 mV) to record EPSC/IPSC sequences and examine E-I windows (Figure 6). Pairing led to a decrease in E-I window duration at multiple holding potentials, both for pre→post pairing (Figures 6A and 6B) and post→pre pairing (Figures 6C and 6D). On a cell-by-cell basis, these decreases in E-I windows were more apparent at depolarized than hyperpolarized potentials, mainly due to the reduction of outward current at hyperpolarized levels. Reductions in EPSC amplitude and overall duration of excitation might contribute to this sharper temporal integration window after post→pre pairing. More importantly, it is likely that inhibitory LTP also shortens this duration after both pre→post pairing and post→pre pairing, enforcing temporal integration of paired inputs and improving spike timing precision.

STDP Normalized Excitatory-Inhibitory Ratio

Coordinated changes to paired EPSCs and IPSCs provide a potential mechanism for regulation of excitatory-inhibitory balance in neural circuits. We noticed that the magnitude of STDP, particularly for inhibition, was highly variable from experiment to experiment (Figure 3). We wondered what factors control this variability in inhibitory STDP, and if weaker inhibitory synapses were specifically strengthened to a greater degree than stronger inhibitory synapses.

To compare the strength of inhibitory synapses across different experiments, we computed the E/I ratio for each cell in which EPSCs and IPSCs were both monitored before and after pairing. The E/I ratio is the amplitude of the somatically recorded mean EPSC divided by the amplitude of the mean IPSC. EPSCs and IPSCs for three representative experiments are shown in Figure 7A. Before pairing, there was considerable heterogeneity in E/I ratio values (from left to right, 2.88, 3.70, and 10.38; Figure 7A), ranging between 0.27 and 12.64 (before pairing mean E/I ratio: 3.12 ± 0.49, median: 1.75, n = 49; Figures 7B and 7C). Surprisingly, E/I ratios after pairing could be substantially different from initial E/I ratio values (after pairing mean E/I ratio for pre→post pairing: 1.75 ± 0.30, median: 1.26, n = 24; after pairing mean E/I ratio for post→pre pairing: 1.54 ± 0.28, median: 0.94, n = 25; Figures 7B and 7C). Importantly, when the E/I ratio was initially high (>2.0), there was a significant

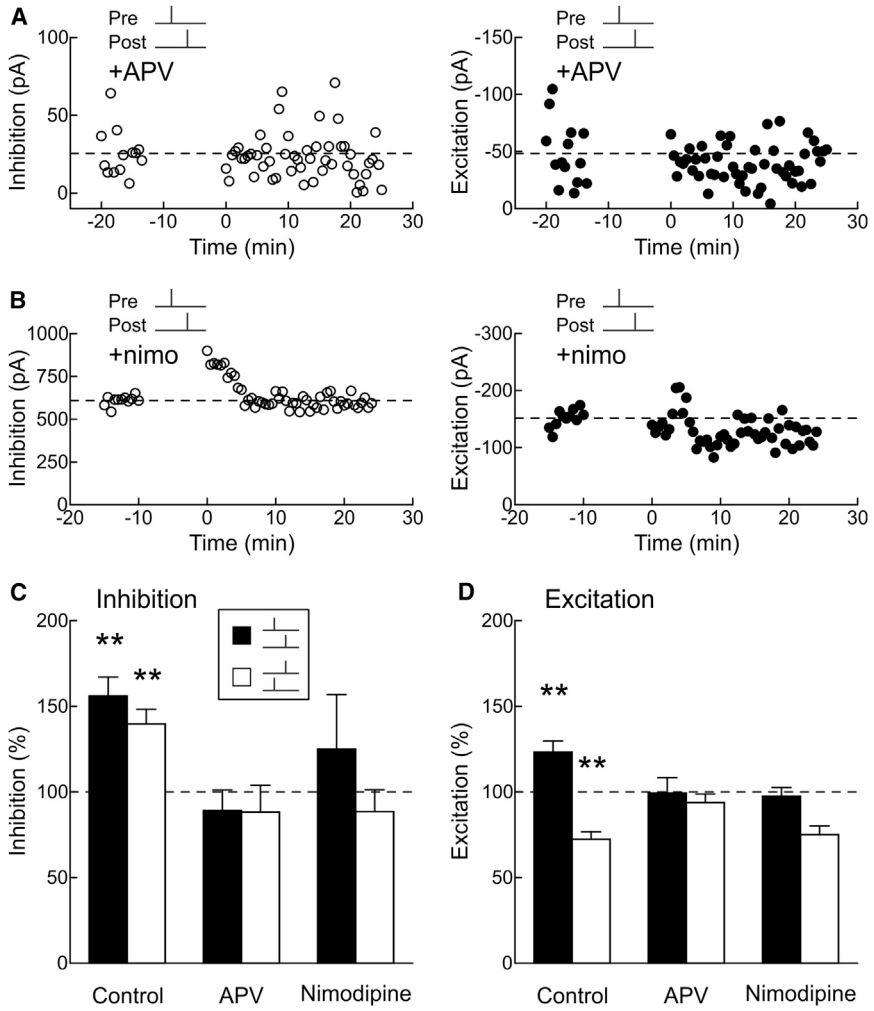

Figure 4. Inhibitory STDP Requires Postsynaptic Ca^{2+} Signaling

(A) Example recording showing that APV (50 μM) prevents induction of inhibitory and excitatory STDP. Left, IPSCs (before, 25.5 ± 4.2 pA; 16–25 min after, 22.2 ± 4.0 pA; change of −13.1%); right, EPSCs (before, −48.2 ± 7.4 pA; after, −40.1 ± 4.1 pA; change of −16.8%); recordings come from the same cell. Spike timing during pre→post pairing: Δt = 3 ms.

(B) Example recording showing that nimodipine (nimo; 15 μM) prevents induction of inhibitory and excitatory STDP. Left, IPSCs (before, 609.3 ± 8.4 pA; after, 600.2 ± 8.7 pA; change of −1.5%); right, EPSCs (before, −151.7 ± 4.7 pA; after, −123.0 ± 4.8 pA, change of −18.9%); recordings come from the same cell. Spike timing during pre→post pairing: Δt = 4 ms.

(C) Summary of pharmacology of inhibitory STDP. Filled bars, short interval pre→post pairing (control, change of 56.2% ± 10.9%, n = 37, $p < 0.0001$; APV, −10.9% ± 12.0%, n = 8, $p > 0.3$; nimodipine, 25.0% ± 32.0%, n = 5, $p > 0.4$). Open bars, short interval post→pre pairing (control, change of 39.7% ± 8.6%, n = 36, $p < 0.0001$; APV, −11.7% ± 15.7%, n = 6, $p > 0.4$; nimodipine, −11.4% ± 12.7%, n = 5, $p > 0.4$). Control cells are both in presence and absence of DNQX. **$p < 0.01$. Error bars represent mean ± SEM.

(D) Pharmacology of excitatory STDP. Filled bars, pre→post pairing (control, change of 23.4% ± 6.4%, n = 46, $p < 0.0002$; APV, −0.6% ± 11.5%, n = 9, $p > 0.9$; nimodipine, −2.4% ± 27.0%, n = 5, $p > 0.9$). Open bars, post→pre pairing (control, change of −27.7% ± 4.4%, n = 38, $p < 0.0001$; APV, −6.2% ± 16.1%, n = 5, $p > 0.7$; nimodipine, −24.8% ± 11.9%, n = 5, $p > 0.1$). Error bars represent mean ± SEM.

reduction in the E/I ratio after pairing for both pre→post pairing and post→pre pairing (Figures 7B and 7C; points to right of vertical red line).

Normalization of E/I ratio may be unsurprising for post→pre pairing experiments in which EPSC amplitudes decreased and IPSC amplitudes increased, acting together to lower E/I ratios. However, pre→post pairing enhances both EPSCs and IPSCs, and should not affect E/I ratios unless excitation and inhibition are differentially modified in a way depending on their initial values. Because there was no significant correlation between the magnitudes of excitatory and inhibitory plasticity induced in each cell (Figure 7D), we instead examined relations between initial synaptic strengths and changes to EPSCs, IPSCs, and E/I ratio (Figures 7E–7J).

We found that the magnitude of inhibitory plasticity was significantly correlated with the initial E/I ratio. In general, excitatory and inhibitory synaptic plasticity was proportional to the initial synaptic strength; i.e., EPSCs and IPSC amplitudes were approximately multiplicatively rescaled after pairing (excitation, Figure 7E; inhibition, Figure 7H). The magnitude of change in excitatory strength was neither related to initial EPSC size (r_+: −0.32, $p > 0.1$; r_-: −0.05, $p > 0.8$; Figure 7F) nor initial E/I ratio (r_+: −0.27, $p > 0.1$; r_-: −0.08, $p > 0.7$; Figure 7G). This was in contrast to the amount of inhibitory plasticity observed in individual experiments. Importantly, while inhibitory plasticity did not depend on initial IPSC size (r_+: −0.09, $p > 0.6$; r_-: −0.33, $p > 0.1$; Figure 7I), it was significantly related to the initial E/I ratio (r_+: 0.76, $p < 0.0001$; r_-: 0.50, $p < 0.02$; Figure 7J).

To examine this relation in more detail, we tested the hypothesis that the E/I ratio during pairing controls the magnitude of inhibitory LTP. In the last set of studies, we adjusted the strength of extracellular stimulation to a new value during pairing as a straightforward way to transiently change the E/I ratio just during the pairing procedure. This stimulation strength was determined at the onset of each recording as the baseline stimulus intensity was selected, and the stimulation strength for pairing was such that the E/I ratio was >150% than that during baseline stimulation. In the cell shown in Figure 8A, baseline stimulation intensity was 5 V for 8 μs, producing an average EPSC of −25.4 pA and an IPSC of 57.6 pA (leading to an E/I ratio of 0.44), whereas during pairing the stimulus intensity was temporarily changed to 5 V for 16 μs to evoke EPSCs of −257.1 pA and IPSCs of 124.6 pA (leading to an E/I ratio of 2.06). After pre→post pairing (Δt: 4 ms), the stimulus intensity

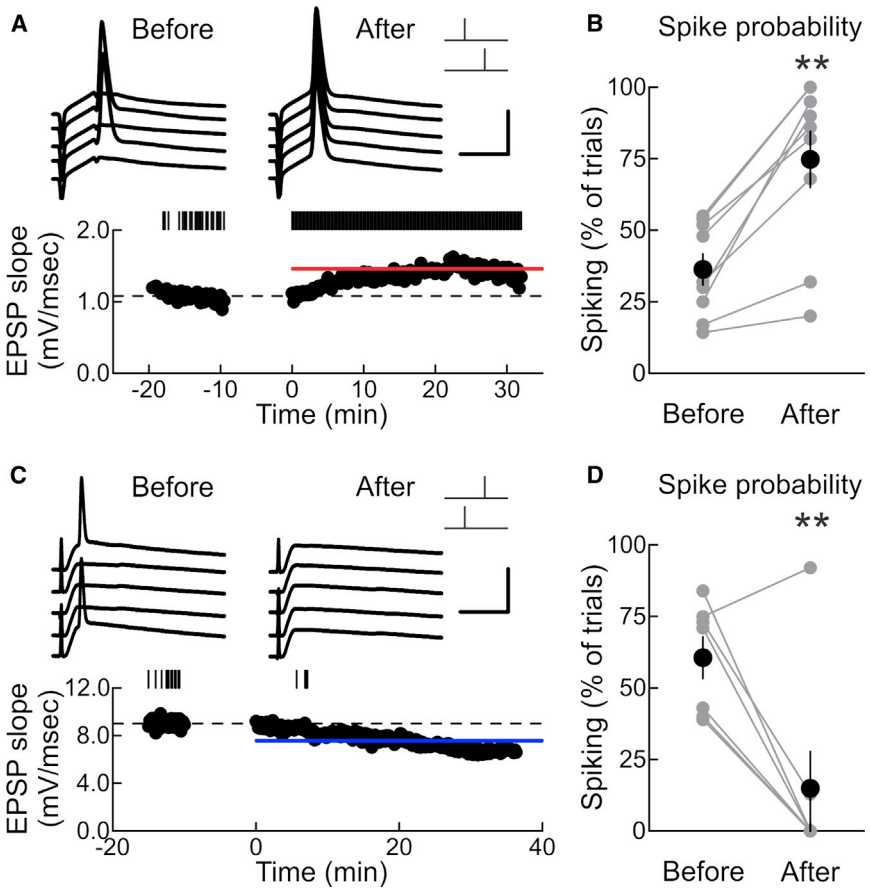

Figure 5. STDP Modifies Spiking Probability

(A) Example current-clamp recording showing increased postsynaptic spike probability after pre→post pairing. Top, example traces before and ~16–25 min after spike pairing. Scale: 5 ms, 50 mV. Bottom, EPSPs before and after pairing. Dashed line, mean EPSP slope before pairing; red bar, mean EPSP slope 16–25 min after pairing (before, 1.08 ± 0.01 mV/ms; after, 1.46 ± 0.01 mV/ms; increase of 35.1%). Upper tick marks show events that also produced a spike; spike probability before pairing: 0.54, spike probability after pairing: 1.0.

(B) Summary of changes to spike probability (before, 0.36 ± 0.05; after, 0.75 ± 0.10; n = 9, $p < 0.0005$; seven of nine cells showed significant increases in spiking) after pre→post pairing. **$p < 0.01$. Error bars represent mean ± SEM.

(C) Example current-clamp recording showing decreased postsynaptic spike probability after post→pre pairing. Scale: 10 ms, 50 mV. Dashed line, mean EPSP slope before pairing; blue bar, mean EPSP slope 16–25 min after pairing (before, 9.01 ± 0.07 mV/ms; after, 7.58 ± 0.04 mV/ms; decrease of −15.8%). Spike probability before pairing, 0.39; spike probability after pairing, 0.0.

(D) Summary of changes to spike probability (before, 0.61 ± 0.07; after, 0.15 ± 0.13; n = 8, $p < 0.01$; seven of eight cells showed significant decreases in spiking) after post→pre pairing. Error bars represent mean ± SEM.

was reset to the baseline level, and 16–25 min later, inhibition had increased to 86.4 ± 1.9 pA.

We asked whether the baseline E/I ratio or the E/I ratio during pairing more accurately determined the amount of inhibitory LTP. We examined the relation between E/I ratios and inhibitory plasticity (Figure 7J), and used the linear fits to those data to make predictions as to the magnitude of inhibitory LTP. For the cell in Figure 8A, the baseline E/I ratio (0.44) predicted inhibitory plasticity of 129.2%, whereas the E/I ratio during pairing (2.06) predicted inhibitory plasticity of 154.7%. The amount of inhibitory plasticity induced was 150.0%, leading to prediction errors of −20.8% for the baseline E/I ratio versus 4.7% for the E/I ratio during pairing.

For the seven cells in which pre→post pairing was performed (Δt: 4 ms in each case), the E/I ratios before and during pairing are displayed in Figure 8B, bottom left; whereas the errors of the predictions based on those ratios are shown in Figure 8B, bottom right. The prediction errors based on the E/I ratios during pairing were significantly lower than those based on the initial E/I ratios. Five of seven of these cells showed significant excitatory LTP, whereas all seven cells showed significant inhibitory LTP.

This was also the case for post→pre pairing (Δt: −4 ms in each case). In the cell shown in Figure 8C, the baseline stimulation strength was 5 V for 12 μs whereas the paired strength was 6 V for 18 μs. The amount of inhibitory LTP induced after pairing was 127.7%, the baseline E/I ratio (0.55) predicted inhibitory plasticity of 114.3% (prediction error: −13.4%), and the E/I ratio during pairing (1.88) predicted inhibitory plasticity of 124.2% (prediction error: −3.5%). The prediction errors of inhibitory plasticity based on the pairing E/I ratios were significantly lower than errors based on baseline E/I ratios over a total of nine post→pre pairing experiments (Figure 8D; six of nine cells showed significant excitatory LTD; nine of nine cells showed significant inhibitory LTP). Thus, inhibitory plasticity acts to normalize excitatory-inhibitory balance and is substantially higher in magnitude when inhibition is weak relative to excitation. Moreover, this indicates that excitatory and inhibitory synapses, however initially disparate and unrelated, become more similar in net somatic strength when linked together by postsynaptic spiking.

DISCUSSION

Inhibitory synaptic strengths must be carefully calibrated with the relative weights of excitatory synapses to ensure that neurons and networks are neither hypo- nor hyper-excitable for prolonged periods (Isaacson and Scanziani, 2011). This balance between excitation and inhibition is a general feature of neural circuits, particularly in the mature auditory cortex (Froemke et al., 2007; Tan and Wehr, 2009; Volkov and Galazjuk, 1991; Wehr and Zador, 2003), visual cortex (Ferster, 1986; Hensch and Fagiolini, 2005; Hirsch et al., 1998), somatosensory cortex

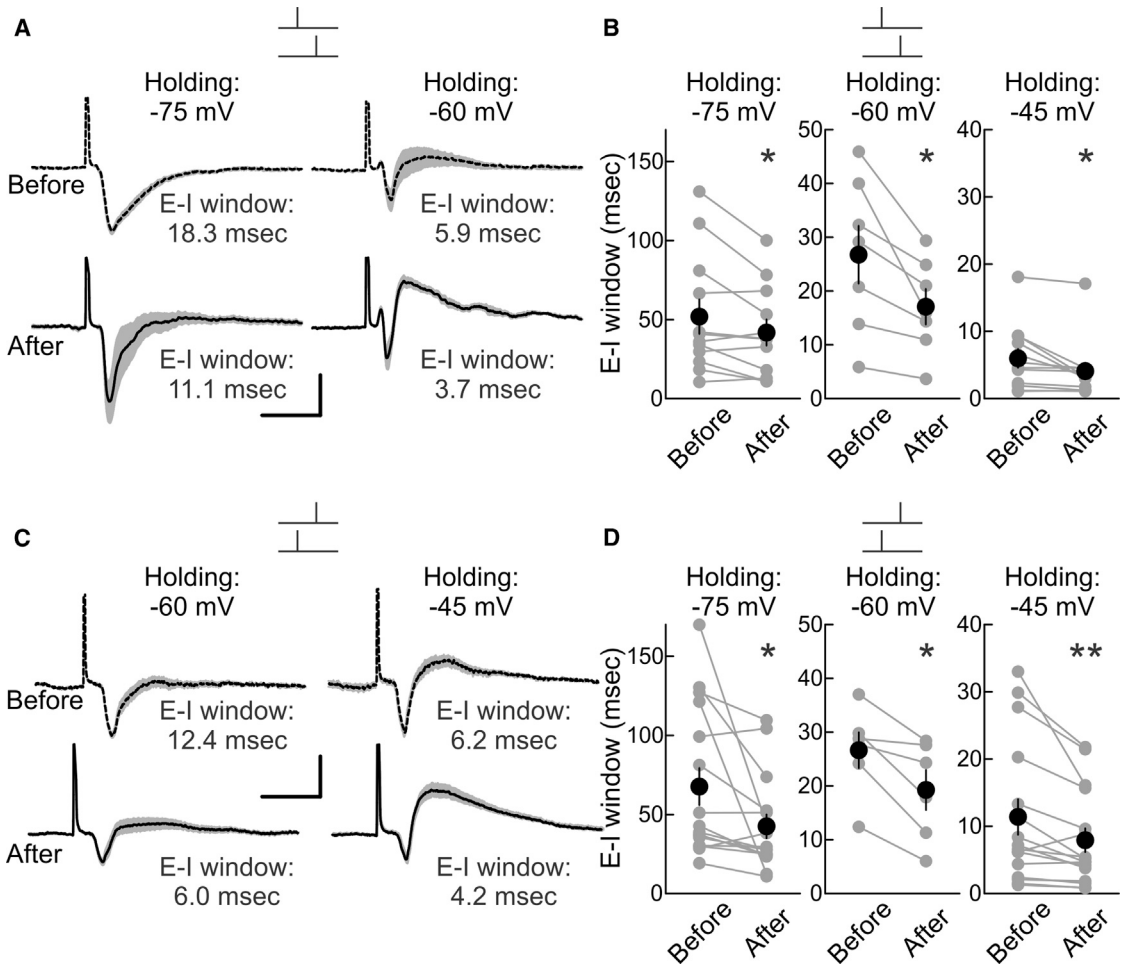

Figure 6. STDP Sharpens Synaptic Integration Window

(A) Example E-I time windows for the same cell before and after pre→post pairing at holding potential of −75 mV (top: E-I window before pairing, 18.3 ms; E-I window after pairing, 11.1 ms) and −60 mV (top: E-I window before pairing, 5.9 ms; E-I window after pairing, 3.7 ms). Scale: 15 ms, 100 pA.

(B) Summary of changes to E-I windows after pre→post pairing, as measured at −75 mV (before, 52.0 ± 10.9 ms; after, 42.0 ± 8.2 ms; n = 12, $p < 0.03$; 3/12 cells showed significant decreases in E-I window), −60 mV (before, 26.9 ± 5.4 ms; after, 17.2 ± 3.3 ms; n = 7, $p < 0.02$; two of seven cells showed significant decreases in E-I window), and −45 mV (before, 6.0 ± 1.4 ms; after, 4.2 ± 1.2 ms; n = 12, $p < 0.02$; 7/12 cells showed significant decreases in E-I window). Error bars represent mean ± SEM.

(C) Example E-I time windows from the same cell (different recording than in A after post→pre pairing at holding potential of −60 mV (bottom: E-I window before pairing, 12.4 ms; E-I window after pairing, 6.0 ms) and −45 mV (top: E-I window before pairing, 6.2 ms; E-I window after pairing, 4.2 ms). Scale: 15 ms, 50 pA.

(D) Summary of changes to E-I windows after post→pre pairing as measured at −75 mV (before, 67.5 ± 11.8 ms; after, 42.4 ± 7.5 ms; n = 16, $p < 0.03$; 9/16 cells showed significant decreases in E-I window), −60 mV (before, 26.7 ± 11.8 ms; after, 19.3 ± 3.7 ms; n = 6, $p < 0.02$; two of six cells showed significant decreases in E-I window), and −45 mV (before, 11.4 ± 2.6 ms; after, 7.9 ± 1.8 ms; n = 16, $p < 0.009$; 12/16 cells showed significant decreases in E-I window). Error bars represent mean ± SEM.

(Higley and Contreras, 2006; Okun and Lampl, 2008), hippocampus (Mann and Paulsen, 2007), and the olfactory system (Didier et al., 2001; Poo and Isaacson, 2009). Excitatory-inhibitory balance in the auditory cortex is likely specific for particular features or receptive field properties, and fine-scale balance of frequency tuning seems to be established during early postnatal development (Dorrn et al., 2010). The tuning properties of inhibitory synapses are susceptible to changes in patterns of sensory experience during this critical period, although it is unknown how adjustments of synaptic frequency tuning (as measured in vivo) relate to synaptic plasticity rules (generally studied in vitro). Inspired by the theoretical investigation of inhibitory STDP by Vogels et al. (2011), we examined the basic circuit mechanisms that regulate inhibitory synaptic strength and excitatory-inhibitory balance in layer 5 neurons of mouse auditory cortex.

Our results show that inhibitory and excitatory synapses are modifiable by a few minutes of coincident single pre- and postsynaptic spiking. Excitatory synapses displayed a typical Hebbian asymmetric STDP time window, with pre→post pairing inducing LTP within ~10 ms and post→pre pairing inducing LTD. In contrast, inhibition was potentiated within ~10 ms of

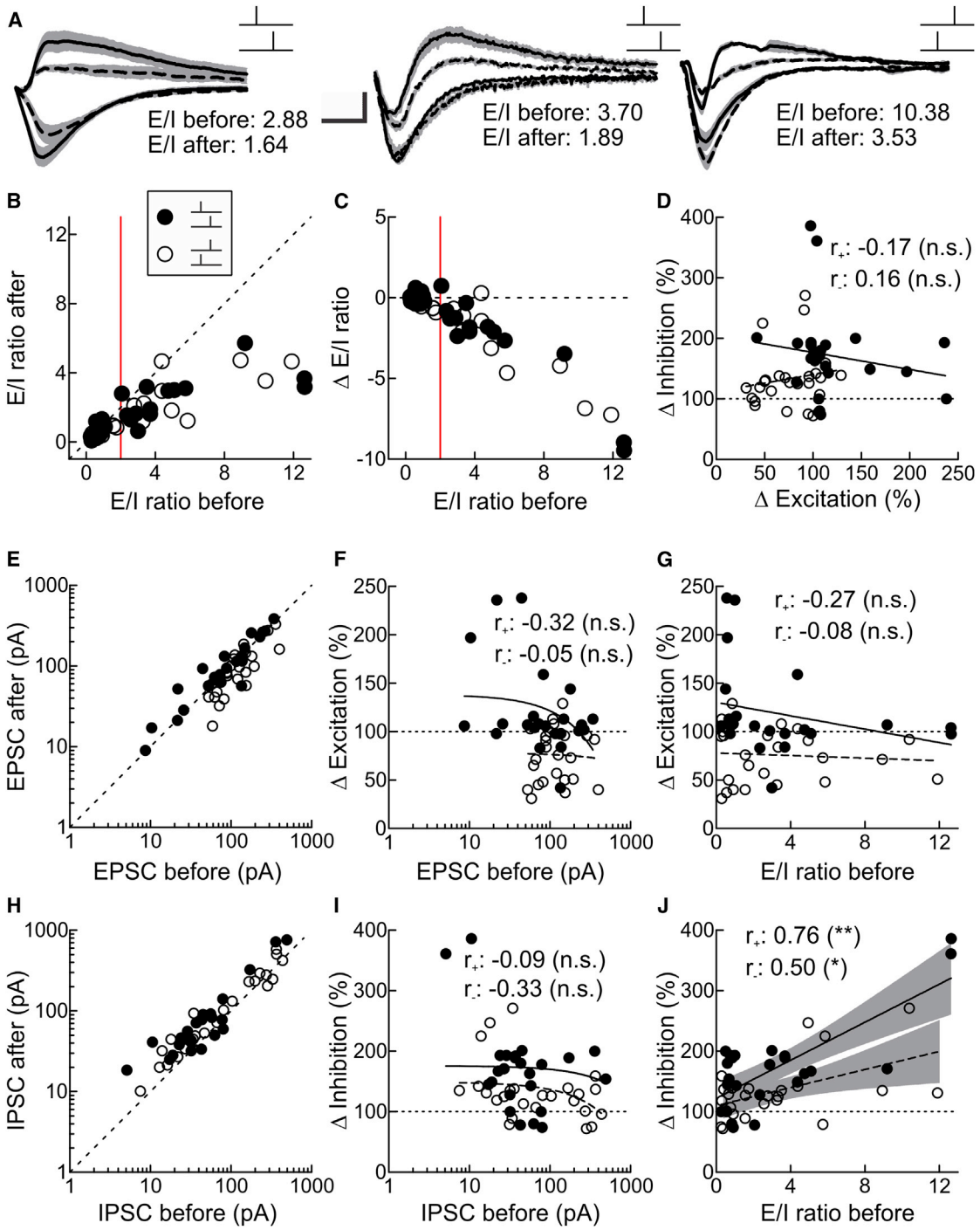

Figure 7. STDP Normalizes Excitatory-Inhibitory Ratio of Paired Inputs

(A) Example neurons showing changes to excitation-inhibition ratio (E/I) after pre→post pairing (left and center) or post→pre pairing (right). Dashed lines, IPSCs and EPSCs before pairing; solid lines, IPSCs and EPSCs after pairing. Gray, SEM of three to five traces per event. Scale: 10 ms, 100 pA (left), 75 pA (middle), 200 pA (right).

(B) E/I ratio before and after pairing for each short pre→post pairing (filled symbols, n = 24) and short post→pre pairing (open symbols, n = 25) experiment. For pre→post pairing experiments where initial E/I ratio was ≤2.0 (red vertical line), E/I ratio before pairing was 0.72 ± 0.07 and E/I ratio after pairing was 0.73 ± 0.11 (n = 12, $p > 0.9$). For pre→post pairing experiments where initial E/I ratio was >2.0, E/I ratio before pairing was 5.53 ± 1.10 and E/I ratio after pairing was 2.77 ± 0.42 (n = 12, $p < 0.02$). For post→pre pairing experiments where initial E/I ratio was ≤2.0, E/I ratio before pairing was 0.79 ± 0.15 and E/I ratio after pairing was 0.51 ± 0.09 (n = 13, $p < 0.008$). For post→pre pairing experiments where initial E/I ratio was >2.0, E/I ratio before pairing was 5.63 ± 0.90 and E/I ratio after pairing was 2.66 ± 0.36 (n = 12, $p < 0.002$).

(legend continued on next page)

postsynaptic spiking regardless of the relative pre/post spike timing. The shape of the experimentally determined inhibitory STDP window is similar but not identical to that used by Vogels et al. (2011), although more recent modeling work has indicated that other variations in inhibitory STDP learning rules might also in principle balance excitation and inhibition (Luz and Shamir, 2012).

Inhibitory plasticity has been described for some other synapses, although the studies of inhibitory plasticity are fewer in number than studies of excitatory plasticity onto excitatory and inhibitory neurons (Lamsa et al., 2010; Vogels et al., 2013). Most previous experimental studies that have examined inhibitory synaptic plasticity were done in the absence of excitatory transmission (Hartmann et al., 2008; Haas et al., 2006; Holmgren and Zilberter, 2001; Maffei et al., 2006). This is useful for understanding the basic mechanisms by which inhibitory synaptic strength can be changed, but different rules and mechanisms may be involved when excitation and inhibition are monitored together. For example, Wang and Maffei (2014) recently found in visual cortex that when inhibitory connections were potentiated, excitatory LTP was suppressed. Additionally, the specific spike timing requirements for inhibitory LTP and LTD may vary depending on synaptic function and/or location. Haas et al. (2006) found an asymmetric window for inhibitory STDP in slices of rat entorhinal cortex that was blocked by nimodipine. Network models indicated that this form of plasticity could also balance inhibition with excitation. Thus, synapse-specific differences in STDP might have additional functional consequences, such as enforcing certain patterns of temporal correlations (Froemke et al., 2005) or sharpening spike timing as observed here in the auditory cortex.

The form of inhibitory plasticity described here in the auditory cortex depends on NMDA receptors, ensuring that inhibitory synapses are modified together with co-activated excitatory synapses by inducing LTP at both excitatory and inhibitory inputs after pre→post pairing. There are other reports of NMDA receptor-dependent inhibitory plasticity (Huang et al., 2005; Ormond and Woodin, 2011; Potapenko et al., 2013), which may require common CaMKII-mediated phosphorylation with co-potentiated excitatory inputs (Huang et al., 2005; Wang et al., 1995) and/or increased numbers of synaptic GABA receptors (Nusser et al., 1998). Future experiments will be required to determine how NMDA receptor signaling interacts with postsynaptic spiking and inhibitory synapses for coordinated induction of excitatory and inhibitory long-term plasticity.

Our focus here was the functional consequences of concomitant excitatory and inhibitory STDP. We found that spike pairing shortened the integration window between excitation and inhibition regardless of the temporal order of pre- and postsynaptic spiking. This suggests that inhibitory STDP enforces spike-timing fidelity by reducing the period during which incoming events are effective in depolarizing postsynaptic neurons. Additionally, STDP increased the reliability of paired inputs evoking action potentials after pre→post pairing, but decreased spike firing probability after post→pre pairing. Because of the lag between excitation and inhibition, these changes in spike generation are likely a direct consequence of excitatory plasticity alone. However, because inhibitory potentiation narrowed the temporal integration window, larger excitatory events after pre→post pairing have a limited period to sum together before larger inhibitory responses are activated.

More importantly, both pre→post pairing and post→pre pairing reduced the E/I ratio of paired inputs when this ratio was large (>2). This occurred irrespective of the precise temporal ordering of presynaptic and postsynaptic spiking. For post→pre pairing, the decrease in E/I ratio is a natural consequence of excitatory and inhibitory plasticity; reductions in E/I ratios could be due to either excitatory LTD and/or inhibitory LTP. However, for pre→post pairing, we found that the E/I ratios were reduced because the magnitude of inhibitory plasticity was larger when the initial E/I excitability ratio was higher. This dependence helps to account for some of the variability in the expression of inhibitory STDP from experiment to experiment.

How might inhibitory synapses be sensitive to the specific E/I ratio during pairing? It is possible that when the E/I ratio is higher, relatively more Ca^{2+} channel and NMDA receptor activation occurs during spike pairing due to the increased level of depolarization. This would then result in greater recruitment of Ca^{2+}-dependent signaling molecules such as CaMKII, found to be important for inhibitory plasticity in hippocampus (Huang et al., 2005). Conversely, lower E/I ratios may mean that inhibition more effectively clamped NMDA receptor responses, limiting the

(C) E/I ratio before pairing versus net change in E/I ratio after pairing, for each short pre→post pairing (filled symbols) and short post→pre pairing (open symbols) experiment. For pre→post pairing experiments where initial E/I ratio was ≤2.0 (red vertical line), E/I ratio changed by 0.00 ± 0.09. For pre→post pairing experiments where initial E/I ratio was >2.0, E/I ratio changed by −2.76 ± 0.93. For post→pre pairing experiments where initial E/I ratio was ≤2.0, E/I ratio changed by −0.29 ± 0.09. For post→pre pairing experiments where initial E/I ratio was >2.0, E/I ratio changed by −2.97 ± 0.67.

(D) Change in inhibition does not depend on change in excitation within each cell, for short pre→post pairing (filled symbols and solid line, r_+: −0.17, $p > 0.6$) or short post→pre pairing (open symbols and dashed line, r_-: 0.16, $p > 0.6$) experiments. n.s., not significant.

(E) EPSC amplitudes for each cell before and after pairing for short pre→post pairing (filled symbols) and short post→pre pairing (open symbols) experiments.

(F) Change in excitation does not depend on initial EPSC amplitude (linear correlation coefficient for pre→post pairing, r_+: −0.25, $p > 0.2$; post→pre pairing, r_-: −0.05, $p > 0.8$).

(G) Change in excitation does not depend on initial E/I ratio (pre → post r_+: −0.32, $p > 0.1$; post → pre r_-: −0.05, $p > 0.8$).

(H) IPSC amplitudes for each cell before and after pairing for short pre→post pairing (filled symbols) and short post→pre pairing (open symbols) experiments.

(I) Change in inhibition does not depend on initial IPSC amplitude (pre → post r_+: −0.09, $p > 0.6$; post → pre r_-: −0.33, $p > 0.1$).

(J) Change in inhibition depends on initial E/I ratio (pre → post r_+: 0.76, $p < 0.0001$; post → pre r_-: 0.50, $p < 0.02$). Shaded region indicates 95% confidence intervals for linear predictions. **$p < 0.001$; *$p < 0.05$.

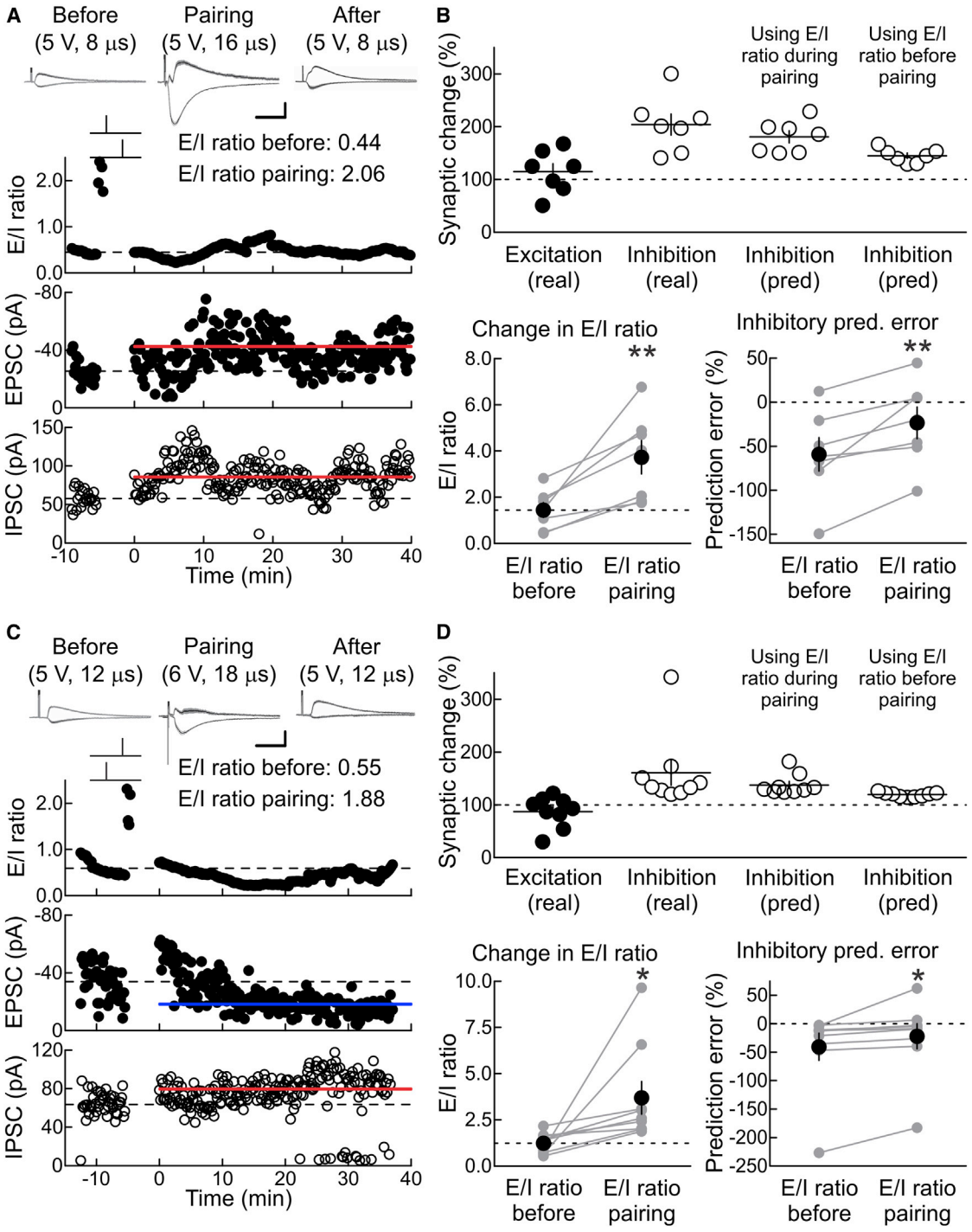

Figure 8. Adjusting E/I Ratio during Pairing Affects Inhibitory STDP

(A) Example recording with transient increase in E/I ratio during pre→post pairing. Top: E/I ratio (before pairing, 0.44; during pairing, 2.06). Middle: EPSCs (before, −25.4 ± 1.6 pA; after, −42.5 ± 1.6 pA; excitatory LTP, 167.4%). Bottom: IPSCs (before, 57.6 ± 2.4 pA; after, 86.4 ± 1.9 pA; inhibitory LTP, 150.0%). E/I ratio before pairing predicted inhibitory LTP of 129.2% (prediction error −20.8%); E/I ratio during pairing predicted inhibitory LTP of 154.7% (prediction error 4.7%).

(B) Summary of experiments increasing E/I ratio during pre→post pairing. Top: E/I ratios (mean E/I ratio before pairing, 1.44 ± 0.32; mean E/I ratio during pairing, 3.72 ± 0.72; n = 7, p < 0.008). Bottom: inhibitory LTP prediction errors (prediction error based on baseline E/I ratios, −59.1% ± 19.0%; prediction error based on higher E/I ratios during pairing, −23.2% ± 18.0%, n = 7, p < 0.008). Five of seven cells showed significant excitatory LTP; seven of seven cells showed significant inhibitory LTP. **p < 0.01. Error bars represent mean ± SEM.

(legend continued on next page)

magnitude of inhibitory plasticity away from the sites of excitatory inputs containing NMDA receptors. Thus regardless of the initial relative strengths (i.e., initial relative tuning) of excitation and inhibition, repetitive spike pairing and STDP act to normalize co-activated excitatory and inhibitory inputs, effectively enhancing their co-tuning together with that of the postsynaptic neuron.

EXPERIMENTAL PROCEDURES

Slice Preparation

All procedures were approved under NYU IACUC protocols. Acute slices of auditory cortex were prepared from P10–26 C57Bl/6 mice. For studies of GABAergic reversal potential, some recordings were made in adult animals aged 2–3 months (Figure S1F). Animals were deeply anesthetized with a 1:1 ketamine/xylazine cocktail and decapitated. The brain was rapidly placed in ice-cold dissection buffer containing 87 NaCl mM, 75 mM sucrose, 2 mM KCl, 1.25 mM NaH_2PO_4, 0.5 mM $CaCl_2$, 7 mM $MgCl_2$, 25 mM $NaHCO_3$, 1.3 mM ascorbic acid, and 10 mM dextrose, bubbled with 95%/5% O_2/CO_2 (pH 7.4). Slices (300–400 μm thick) were prepared with a vibratome (Leica), placed in warm dissection buffer (33°C–35°C) for <30 min, then transferred to a holding chamber containing artificial cerebrospinal fluid at room temperature (ACSF: 124 mM NaCl, 2.5 mM KCl, 1.5 mM $MgSO_4$, 1.25 mM NaH_2PO_4, 2.5 mM $CaCl_2$, and 26 mM $NaHCO_3$,). Slices were kept at room temperature (22°C–24°C) for at least 30 min before use. For experiments, slices were transferred to the recording chamber and perfused (2–2.5 ml/min) with oxygenated ACSF at 33°C.

Electrophysiology

Somatic whole-cell recordings were made from layer 5 pyramidal cells in current-clamp and voltage-clamp mode with a Multiclamp 700B amplifier (Molecular Devices) using IR-DIC video microscopy (Olympus). Patch pipettes (3–8 MΩ) were filled with intracellular solution either for STDP experiments (135 mM K-gluconate, 5 mM NaCl, 10 mM HEPES, 5 mM MgATP, 10 mM phosphocreatine, and 0.3 mM GTP) or voltage-clamp experiments to measure reversal potentials (130 mM Cs-methanesulfonate, 1 mM QX-314, 4 mM TEA-Cl, 0.5 mM BAPTA, 4 mM MgATP, 10 mM phosphocreatine, and 10 mM HEPES, pH 7.2). The mean resting potential was −68.2 ± 5.3 mV (SD). The mean series resistance was 19.7 ± 14.2 MΩ, and the mean input resistance (Ri) was 193.9 ± 99.7 MΩ, determined by monitoring cells with hyperpolarizing pulses (50 pA or 5 mV for 100 ms). Recordings were excluded from analysis if R_i changed >30% compared to the baseline period. Data were filtered at 2 kHz, digitized at 10 kHz, and analyzed with Clampfit 10 (Molecular Devices). Focal extracellular stimulation (0.033–0.2 Hz) was applied with either a bipolar glass electrode (Grass, stimulation strengths of 5–150 μA for 0.01–1.0 ms) or a monopolar metal electrode (AMPI Master-9, stimulation strengths of 0–10 V for 6–30 μs) located 100–150 μm from the recording electrode. EPSP initial slope (first 2 ms) or mean peak EPSC (2 ms window) was used to measure excitatory strength. For inhibitory currents, a larger window (5–20 ms) was used. Stable baselines of synaptic strength were established by 5–20 min of stimulation. Synaptic strength after induction was measured 16–25 min after the end of the induction protocol. To determine whether these changes were significant for individual recordings, we used Student's unpaired two-tailed t tests to compare synaptic strengths before and after pairing for each cell, or Fisher's exact test for changes of spike generation in Figure 5. During induction, postsynaptic spiking was evoked with brief depolarizing current pulses. Presynaptic spike timing was defined as EPSP onset, and postsynaptic spike timing was measured at the peak of the action potential.

The predicted amounts of inhibitory plasticity in Figure 8 were computed from the linear fits to Figure 7J. For pre→post pairing, the linear fit is described by: $y = (15.72 * x) + 122.3$, where x is the E/I ratio (either before or during pairing) and y is the predicted amount of inhibitory plasticity. For post→pre pairing, the linear fit is described by: $y = (7.46 * x) + 110.2$. The prediction error is simply the difference between the predicted and experimentally observed amount of inhibitory plasticity for each cell.

All statistics and error bars are reported as means ± SEM and statistical significance assessed with paired two-tailed Student's t test, unless otherwise noted.

SUPPLEMENTAL INFORMATION

Supplemental Information includes two figures and can be found with this article online at http://dx.doi.org/10.1016/j.neuron.2015.03.014.

AUTHOR CONTRIBUTIONS

J.A.D. and R.C.F. designed the study and wrote the paper. J.A.D. performed the experiments and analyzed the data.

ACKNOWLEDGMENTS

We thank J. Barger, I. Carcea, G. Fishell, M. Jin, K.V. Kuchibhotla, M.A. Long, I. Ninan, R. Tremblay, R.W. Tsien, and N. Zaika for comments, discussions, and technical assistance. This work was funded by grants from NIDCD (DC009635 and DC012557), a Sloan Research Fellowship, and a Klingenstein Fellowship to R.C.F.

Received: June 2, 2014
Revised: November 26, 2014
Accepted: February 11, 2015
Published: April 2, 2015

REFERENCES

Bell, C.C., Han, V.Z., Sugawara, Y., and Grant, K. (1997). Synaptic plasticity in a cerebellum-like structure depends on temporal order. Nature *387*, 278–281.

Bi, G.Q., and Poo, M.M. (1998). Synaptic modifications in cultured hippocampal neurons: dependence on spike timing, synaptic strength, and postsynaptic cell type. J. Neurosci. *18*, 10464–10472.

Bienenstock, E.L., Cooper, L.N., and Munro, P.W. (1982). Theory for the development of neuron selectivity: orientation specificity and binocular interaction in visual cortex. J. Neurosci. *2*, 32–48.

Bliss, T.V.P., and Collingridge, G.L. (1993). A synaptic model of memory: long-term potentiation in the hippocampus. Nature *361*, 31–39.

Buonomano, D.V., and Merzenich, M.M. (1998). Cortical plasticity: from synapses to maps. Annu. Rev. Neurosci. *21*, 149–186.

Carcea, I., and Froemke, R.C. (2013). Cortical plasticity, excitatory-inhibitory balance, and sensory perception. Prog. Brain Res. *207*, 65–90.

Chang, E.F., Bao, S., Imaizumi, K., Schreiner, C.E., and Merzenich, M.M. (2005). Development of spectral and temporal response selectivity in the auditory cortex. Proc. Natl. Acad. Sci. USA *102*, 16460–16465.

(C) Example recording with transient increase in E/I ratio during post→pre pairing. Top: E/I ratio (before pairing, 0.55; during pairing, 1.88). Middle: EPSCs (before, −33.9 ± 1.9 pA; after, −18.3 ± 0.7 pA; excitatory LTD, −46.0%). Bottom: IPSCs (before, 62.4 ± 2.4 pA; after, 79.7 ± 2.1 pA; inhibitory LTP, 127.7%). E/I ratio before pairing predicted inhibitory LTP of 114.3% (prediction error −13.4%); E/I ratio during pairing predicted inhibitory LTP of 124.2% (prediction error −3.5%).

(D) Summary of experiments increasing E/I ratio during post→pre pairing. Top: E/I ratios (mean E/I ratio before pairing, 1.24 ± 0.19; mean E/I ratio during pairing, 3.70 ± 0.89; n = 9, $p < 0.04$). Bottom: inhibitory LTP prediction errors (prediction error based on baseline E/I ratios, −41.2% ± 23.7%; prediction error based on higher E/I ratios during pairing, −22.8% ± 22.1%; n = 9, $p < 0.04$). Six of nine cells showed significant excitatory LTD; nine of nine cells showed significant inhibitory LTP. *$p < 0.05$. Error bars represent mean ± SEM.

Dan, Y., and Poo, M.M. (2006). Spike timing-dependent plasticity: from synapse to perception. Physiol. Rev. *86*, 1033–1048.

de Villers-Sidani, E., Chang, E.F., Bao, S., and Merzenich, M.M. (2007). Critical period window for spectral tuning defined in the primary auditory cortex (A1) in the rat. J. Neurosci. *27*, 180–189.

Debanne, D., Gähwiler, B.H., and Thompson, S.M. (1994). Asynchronous pre- and postsynaptic activity induces associative long-term depression in area CA1 of the rat hippocampus in vitro. Proc. Natl. Acad. Sci. USA *91*, 1148–1152.

DeFelipe, J., López-Cruz, P.L., Benavides-Piccione, R., Bielza, C., Larrañaga, P., Anderson, S., Burkhalter, A., Cauli, B., Fairén, A., Feldmeyer, D., et al. (2013). New insights into the classification and nomenclature of cortical GABAergic interneurons. Nat. Rev. Neurosci. *14*, 202–216.

Didier, A., Carleton, A., Bjaalie, J.G., Vincent, J.D., Ottersen, O.P., Storm-Mathisen, J., and Lledo, P.M. (2001). A dendrodendritic reciprocal synapse provides a recurrent excitatory connection in the olfactory bulb. Proc. Natl. Acad. Sci. USA *98*, 6441–6446.

Dorrn, A.L., Yuan, K., Barker, A.J., Schreiner, C.E., and Froemke, R.C. (2010). Developmental sensory experience balances cortical excitation and inhibition. Nature *465*, 932–936.

Feldman, D.E. (2000). Timing-based LTP and LTD at vertical inputs to layer II/III pyramidal cells in rat barrel cortex. Neuron *27*, 45–56.

Feldman, D.E. (2012). The spike-timing dependence of plasticity. Neuron *75*, 556–571.

Ferster, D. (1986). Orientation selectivity of synaptic potentials in neurons of cat primary visual cortex. J. Neurosci. *6*, 1284–1301.

Fishell, G., and Rudy, B. (2011). Mechanisms of inhibition within the telencephalon: "where the wild things are". Annu. Rev. Neurosci. *34*, 535–567.

Frankland, P.W., O'Brien, C., Ohno, M., Kirkwood, A., and Silva, A.J. (2001). α-CaMKII-dependent plasticity in the cortex is required for permanent memory. Nature *411*, 309–313.

Froemke, R.C., and Dan, Y. (2002). Spike-timing-dependent synaptic modification induced by natural spike trains. Nature *416*, 433–438.

Froemke, R.C., and Martins, A.R. (2011). Spectrotemporal dynamics of auditory cortical synaptic receptive field plasticity. Hear. Res. *279*, 149–161.

Froemke, R.C., Poo, M.M., and Dan, Y. (2005). Spike-timing-dependent synaptic plasticity depends on dendritic location. Nature *434*, 221–225.

Froemke, R.C., Merzenich, M.M., and Schreiner, C.E. (2007). A synaptic memory trace for cortical receptive field plasticity. Nature *450*, 425–429.

Froemke, R.C., Debanne, D., and Bi, G.Q. (2010). Temporal modulation of spike-timing-dependent plasticity. Front Synaptic Neurosci *2*, 19.

Froemke, R.C., Carcea, I., Barker, A.J., Yuan, K., Seybold, B.A., Martins, A.R., Zaika, N., Bernstein, H., Wachs, M., Levis, P.A., Polley, D.B., Merzenich, M.M., and Schreiner, C.E. (2013). Long-term modification of cortical synapses improves sensory perception. Nat. Neurosci. *16*, 79–88.

Gaiarsa, J.L., Caillard, O., and Ben-Ari, Y. (2002). Long-term plasticity at GABAergic and glycinergic synapses: mechanisms and functional significance. Trends Neurosci. *25*, 564–570.

Gil, Z., and Amitai, Y. (1996). Properties of convergent thalamocortical and intracortical synaptic potentials in single neurons of neocortex. J. Neurosci. *16*, 6567–6578.

Haas, J.S., Nowotny, T., and Abarbanel, H.D. (2006). Spike-timing-dependent plasticity of inhibitory synapses in the entorhinal cortex. J. Neurophysiol. *96*, 3305–3313.

Hartmann, K., Bruehl, C., Golovko, T., and Draguhn, A. (2008). Fast homeostatic plasticity of inhibition via activity-dependent vesicular filling. PLoS ONE *3*, e2979.

Hebb, D.O. (1949). The Organization of Behavior. (Wiley).

Hensch, T.K., and Fagiolini, M. (2005). Excitatory-inhibitory balance and critical period plasticity in developing visual cortex. Prog. Brain Res. *147*, 115–124.

Higley, M.J., and Contreras, D. (2006). Balanced excitation and inhibition determine spike timing during frequency adaptation. J. Neurosci. *26*, 448–457.

Hirsch, J.A., Alonso, J.M., Reid, R.C., and Martinez, L.M. (1998). Synaptic integration in striate cortical simple cells. J. Neurosci. *18*, 9517–9528.

Holmgren, C.D., and Zilberter, Y. (2001). Coincident spiking activity induces long-term changes in inhibition of neocortical pyramidal cells. J. Neurosci. *21*, 8270–8277.

Huang, C.S., Shi, S.H., Ule, J., Ruggiu, M., Barker, L.A., Darnell, R.B., Jan, Y.N., and Jan, L.Y. (2005). Common molecular pathways mediate long-term potentiation of synaptic excitation and slow synaptic inhibition. Cell *123*, 105–118.

Isaacson, J.S., and Scanziani, M. (2011). How inhibition shapes cortical activity. Neuron *72*, 231–243.

Kirkwood, A., Dudek, S.M., Gold, J.T., Aizenman, C.D., and Bear, M.F. (1993). Common forms of synaptic plasticity in the hippocampus and neocortex in vitro. Science *260*, 1518–1521.

Komatsu, Y. (1994). Age-dependent long-term potentiation of inhibitory synaptic transmission in rat visual cortex. J. Neurosci. *14*, 6488–6499.

Kruglikov, I., and Rudy, B. (2008). Perisomatic GABA release and thalamocortical integration onto neocortical excitatory cells are regulated by neuromodulators. Neuron *58*, 911–924.

Kullmann, D.M., Moreau, A.W., Bakiri, Y., and Nicholson, E. (2012). Plasticity of inhibition. Neuron *75*, 951–962.

Lamsa, K.P., Kullmann, D.M., and Woodin, M.A. (2010). Spike-timing dependent plasticity in inhibitory circuits. Front Synaptic Neurosci *2*, 8.

Letzkus, J.J., Wolff, S.B.E., Meyer, E.M.M., Tovote, P., Courtin, J., Herry, C., and Lüthi, A. (2011). A disinhibitory microcircuit for associative fear learning in the auditory cortex. Nature *480*, 331–335.

Luhmann, H.J., and Prince, D.A. (1991). Postnatal maturation of the GABAergic system in rat neocortex. J. Neurophysiol. *65*, 247–263.

Luz, Y., and Shamir, M. (2012). Balancing feed-forward excitation and inhibition via Hebbian inhibitory synaptic plasticity. PLoS Comput. Biol. *8*, e1002334.

Maffei, A., Nataraj, K., Nelson, S.B., and Turrigiano, G.G. (2006). Potentiation of cortical inhibition by visual deprivation. Nature *443*, 81–84.

Malenka, R.C., and Nicoll, R.A. (1999). Long-term potentiation—a decade of progress? Science *285*, 1870–1874.

Mann, E.O., and Paulsen, O. (2007). Role of GABAergic inhibition in hippocampal network oscillations. Trends Neurosci. *30*, 343–349.

Markram, H., Lübke, J., Frotscher, M., and Sakmann, B. (1997). Regulation of synaptic efficacy by coincidence of postsynaptic APs and EPSPs. Science *275*, 213–215.

Markram, H., Gerstner, W., and Sjöström, P.J. (2011). A history of spike-timing-dependent plasticity. Front Synaptic Neurosci *3*, 4.

Martin, S.J., Grimwood, P.D., and Morris, R.G. (2000). Synaptic plasticity and memory: an evaluation of the hypothesis. Annu. Rev. Neurosci. *23*, 649–711.

McClelland, J.L., McNaughton, B.L., and O'Reilly, R.C. (1995). Why there are complementary learning systems in the hippocampus and neocortex: insights from the successes and failures of connectionist models of learning and memory. Psychol. Rev. *102*, 419–457.

McGaugh, J.L. (2000). Memory—a century of consolidation. Science *287*, 248–251.

Metherate, R., and Ashe, J.H. (1993). Nucleus basalis stimulation facilitates thalamocortical synaptic transmission in the rat auditory cortex. Synapse *14*, 132–143.

Nusser, Z., Hájos, N., Somogyi, P., and Mody, I. (1998). Increased number of synaptic $GABA(_A)$ receptors underlies potentiation at hippocampal inhibitory synapses. Nature *395*, 172–177.

Okun, M., and Lampl, I. (2008). Instantaneous correlation of excitation and inhibition during ongoing and sensory-evoked activities. Nat. Neurosci. *11*, 535–537.

Ormond, J., and Woodin, M.A. (2011). Disinhibition-mediated LTP in the hippocampus is synapse specific. Front. Cell. Neurosci. *5*, 17.

Owens, D.F., Boyce, L.H., Davis, M.B., and Kriegstein, A.R. (1996). Excitatory GABA responses in embryonic and neonatal cortical slices demonstrated by gramicidin perforated-patch recordings and calcium imaging. J. Neurosci. *16*, 6414–6423.

Poo, C., and Isaacson, J.S. (2009). Odor representations in olfactory cortex: "sparse" coding, global inhibition, and oscillations. Neuron *62*, 850–861.

Potapenko, E.S., Biancardi, V.C., Zhou, Y., and Stern, J.E. (2013). Astrocytes modulate a postsynaptic NMDA-GABAA-receptor crosstalk in hypothalamic neurosecretory neurons. J. Neurosci. *33*, 631–640.

Sjöström, P.J., Turrigiano, G.G., and Nelson, S.B. (2001). Rate, timing, and cooperativity jointly determine cortical synaptic plasticity. Neuron *32*, 1149–1164.

Tan, A.Y., and Wehr, M. (2009). Balanced tone-evoked synaptic excitation and inhibition in mouse auditory cortex. Neuroscience *163*, 1302–1315.

Vogels, T.P., Sprekeler, H., Zenke, F., Clopath, C., and Gerstner, W. (2011). Inhibitory plasticity balances excitation and inhibition in sensory pathways and memory networks. Science *334*, 1569–1573.

Vogels, T.P., Froemke, R.C., Doyon, N., Gilson, M., Haas, J.S., Liu, R., Maffei, A., Miller, P., Wierenga, C.J., Woodin, M.A., et al. (2013). Inhibitory synaptic plasticity: spike timing-dependence and putative network function. Front Neural Circuits *7*, 119.

Volkov, I.O., and Galazjuk, A.V. (1991). Formation of spike response to sound tones in cat auditory cortex neurons: interaction of excitatory and inhibitory effects. Neuroscience *43*, 307–321.

Wang, L., and Maffei, A. (2014). Inhibitory plasticity dictates the sign of plasticity at excitatory synapses. J. Neurosci. *34*, 1083–1093.

Wang, R.A., Cheng, G., Kolaj, M., and Randić, M. (1995). Alpha-subunit of calcium/calmodulin-dependent protein kinase II enhances gamma-aminobutyric acid and inhibitory synaptic responses of rat neurons in vitro. J. Neurophysiol. *73*, 2099–2106.

Wehr, M., and Zador, A.M. (2003). Balanced inhibition underlies tuning and sharpens spike timing in auditory cortex. Nature *426*, 442–446.

Woodin, M.A., Ganguly, K., and Poo, M.M. (2003). Coincident pre- and postsynaptic activity modifies GABAergic synapses by postsynaptic changes in Cl- transporter activity. Neuron *39*, 807–820.